

# Infrared Multiple-Photon Dissociation of the Acetone Enol Radical Cation. Dependence of Nonstatistical Dissociation on Internal Energy

Thomas H. Osterheld and John I. Brauman\*

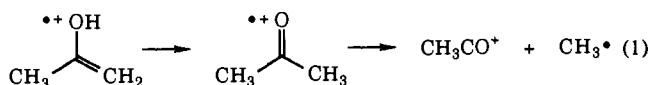
Contribution from the Department of Chemistry, Stanford University, Stanford, California 94305-5080

Received August 10, 1992. Revised Manuscript Received May 19, 1993\*

**Abstract:** Infrared multiple-photon dissociation experiments were used to study the energy dependence of the nonstatistical dissociation of the acetone enol cation. This ion isomerizes to the acetone cation, which then loses its methyl groups at unequal rates. We show that the nonstatistical dissociation increases significantly with the energy in excess of the isomerization barrier. The implication is that excitation of a mode (other than the reaction coordinate), in the transition state for isomerization of the acetone enol cation to the acetone cation, affects the amount of nonstatistical reaction.

A little over 20 years ago Rynbrandt and Rabinovitch published a classical series of papers in which they demonstrated nonergodic reaction behavior.<sup>1,2</sup> Their system involved chemically activating hexafluorobicyclopentane in one of the cyclopentane rings and observing preferential reaction of the initially excited ring. They proposed that some molecules reacted before intramolecular vibrational energy redistribution (ivv) could randomize the energy between both rings.

At about the same time McLafferty and co-workers published a similar proposal for a chemically activated acetone cation.<sup>3,4</sup> This work has never gained as wide acceptance as the Rynbrandt and Rabinovitch study because of questions<sup>5-7</sup> concerning the reaction system and because it is conceptually more difficult, in McLafferty's system, to understand the nonrandom decomposition. The basic reaction mechanism proposed by McLafferty and co-workers has been repeatedly confirmed,<sup>8-19</sup> as has been the observation of nonstatistical reactivity.<sup>8-19</sup> Equation 1 gives the reaction mechanism for dissociation of the acetone enol cation, and Figure 1 gives the generally accepted potential energy surface.<sup>3,18-21</sup>



It is proposed that the acetone enol cation isomerizes to the "symmetric" acetone cation structure, which, then, preferentially

- \* Abstract published in *Advance ACS Abstracts*, October 1, 1993.  
 (1) Rynbrandt, J. D.; Rabinovitch B. S. *J. Chem. Phys.* **1971**, *54*, 2275.  
 (2) Rynbrandt, J. D.; Rabinovitch B. S. *J. Phys. Chem.* **1971**, *75*, 2164.  
 (3) McLafferty, F. W.; McAdoo, D. J.; Smith, J. S.; Kornfeld, R. *J. Am. Chem. Soc.* **1971**, *93*, 3720.  
 (4) McAdoo, D. J.; McLafferty, F. W.; Smith, J. S. *J. Am. Chem. Soc.* **1970**, *92*, 6343.  
 (5) Heyer, R. C.; Russell, M. E. *Org. Mass Spectrom.* **1981**, *16*, 236.  
 (6) Bombach, R.; Stadelmann, J.-P.; Vogt, J. *Chem. Phys.* **1982**, *72*, 259.  
 (7) Johnson, K.; Powis, I.; Danby, C. *J. Chem. Phys.* **1981**, *63*, 1.  
 (8) Turecek, F.; McLafferty, F. W. *J. Am. Chem. Soc.* **1984**, *106*, 2525.  
 (9) Turecek, F.; McLafferty, F. W. *J. Am. Chem. Soc.* **1984**, *106*, 2528.  
 (10) McAdoo, D. J.; Hudson, C. E. *Int. J. Mass Spectrom. Ion Phys.* **1984**, *59*, 77.  
 (11) Turecek, F.; Hanus, V. *Org. Mass Spectrom.* **1984**, *19*, 631.  
 (12) Heinrich, N.; Louage, F.; Lifshitz, C.; Schwarz, H. *J. Am. Chem. Soc.* **1988**, *110*, 8183.  
 (13) Lifshitz, C.; Tzidony, E. *Int. J. Mass Spectrom.* **1981**, *39*, 181.  
 (14) Lifshitz, C. *J. Mass Spectrom. Ion Phys.* **1982**, *43*, 179.  
 (15) Depke, G.; Lifshitz, C.; Schwarz, H.; Tzidony, E. *Angew. Chem., Int. Ed. Engl.* **1981**, *20*, 792.  
 (16) McAdoo, D. J.; Witiak, D. N. *J. Chem. Soc., Perkin Trans. 2* **1981**, 770.  
 (17) McAdoo, D. J. *J. Chem. Phys.* **1983**, *80*, 203.  
 (18) Lifshitz, C.; Berger, P.; Tzidony, E. *Chem. Phys. Lett.* **1983**, *95*, 109.  
 (19) Lifshitz, C. *J. Phys. Chem.* **1983**, *87*, 2304.

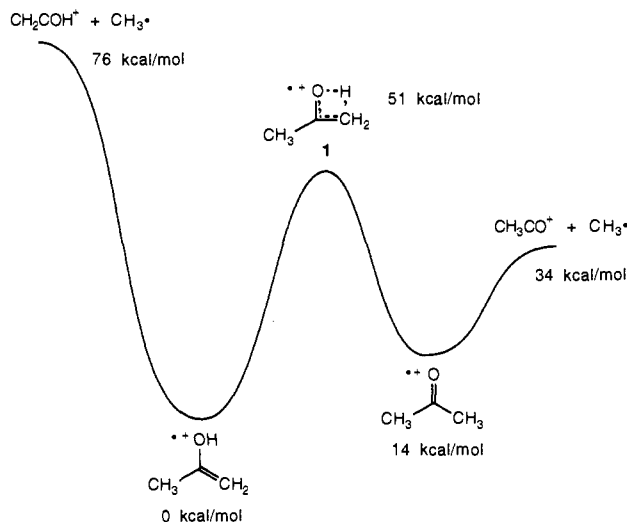


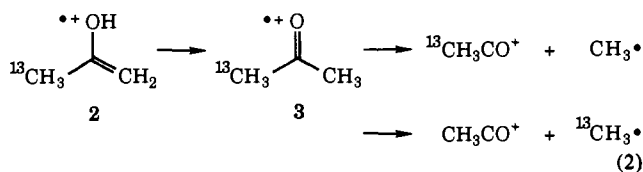
**Figure 1.** Potential energy surface for dissociation of the acetone enol cation. Relative energies are taken from refs 18-21.

loses the newly formed methyl group.<sup>8-19</sup> Metastable-ion experiments<sup>5,8,15</sup> give a selectivity of about 1.4-1. Studies using collisional activation,<sup>8-10</sup> electron impact,<sup>11</sup> chemical reactivity,<sup>22</sup> *ab initio* calculations,<sup>12,23,24</sup> and thermodynamic determinations<sup>11,18,20</sup> are consistent with this mechanism and are not consistent with any of the obvious alternative mechanisms.

The previous studies of the acetone enol cation have involved electron impact induced fragmentation, which was usually studied in the metastable ion<sup>25</sup> time frame. The nature of the activation in previous experiments leaves questions about the energy of reacting species, including the possibility of participation of electronically excited states. We report here the use of infrared multiple-photon (IRMP) dissociation<sup>26-30</sup> to activate 2 with vi-

- (20) Holmes, J. L.; Lossing, F. P. *J. Am. Chem. Soc.* **1982**, *104*, 2048.  
 (21) Trott, W. M.; Blais, N. C.; Walters, E. A. *J. Chem. Phys.* **1978**, *69*, 3150.  
 (22) Diekman, J.; MacLeod, J. K.; Djerassi, C.; Baldeschwieler, J. D. *J. Am. Chem. Soc.* **1969**, *91*, 2069.  
 (23) Bouma, W. J.; MacLeod, J. K.; Radom, L. *J. Am. Chem. Soc.* **1980**, *102*, 2246.  
 (24) Nobes, R. H.; Bouma, W. J.; Radom, L. *J. Am. Chem. Soc.* **1983**, *105*, 309.  
 (25) Cooks, R. G.; Beynon, J. H.; Caprioli, R. M.; Lester, G. R. *Metastable Ions*; Elsevier Scientific Publishing Co.: New York, 1973.  
 (26) Lupo, D. W.; Quack, M. *Chem. Rev.* **1987**, *87*, 181.  
 (27) Quack, M. *J. Chem. Phys.* **1978**, *69*, 1282.  
 (28) Quack, M.; Seyfang, F. *J. Chem. Phys.* **1982**, *76*, 955.

brational energy in order to induce reaction 2 near its threshold.



We confirm the nonstatistical reaction behavior. We also rule out the intervention of an electronically excited state of the acetone cation<sup>19</sup> and most importantly reveal, clearly, the effect of internal energy on the relative rate of the nonstatistical process. These experiments show for the first time that the branching ratio for the nonstatistical reaction has a surprisingly *strong* dependence on the energy above the isomerization transition state (structure 1 in Figure 1). The strong energy dependence suggests that the mechanism for nonstatistical reaction is more complicated than one might have expected. It appears that populating higher energy levels of a mode in 1 (other than the reaction coordinate) increases the nonstatistical reactivity.

### Experimental Section

**Materials.** 1-([<sup>13</sup>C]Methyl)cyclobutanol was synthesized by adding cyclobutanone to an ether solution of <sup>13</sup>CH<sub>3</sub>MgI followed by a normal Grignard workup using an initial wash with an NH<sub>4</sub>Cl solution. The ether was evaporated under vacuum, and then 1-([<sup>13</sup>C]methyl)cyclobutanol was isolated by preparatory gas chromatography on an SE-30 column at 90 °C. Low-energy electron impact on 1-([<sup>13</sup>C]methyl)cyclobutanol<sup>3,22</sup> gives 2 (the <sup>13</sup>C-labeled acetone enol cation) as the main product. Samples were degassed by several freeze-pump-thaw cycles prior to introduction into the high-vacuum system.

**Experiment.** Ions were made, trapped, and detected with a Fourier transform mass spectrometer<sup>31–33</sup> (FT-MS) using the OMEGA data system from IonSpec. The system is equipped with both chirp excitation and the IonSpec impulse excitation.<sup>34–36</sup> We detected the ions with impulse excitation because it gives more accurate isotope ratios and more stable signals. Ions were formed by electron impact ionization at low energies (about 14–17 eV), and then unwanted ions were ejected by standard notched ejection techniques. The ion of interest was then photolyzed by either a CW or a pulsed CO<sub>2</sub> laser, followed by detection. Photolysis scans were compared to scans with the laser blocked to verify that we had mass balance and to correct for any background chemical ionization.

The FT-MS cell is contained in a home-built vacuum system capable of background pressures less than 1 × 10<sup>-8</sup> Torr. Neutral pressures were measured with a nude ionization gauge. The pressures are not corrected; the absolute values are not critical to this study. Neutral ion precursors or reactant species enter through Varian sapphire leak valves. Laser light can enter the vacuum system through a Harshaw 50 mm × 3 mm KCl window located at the front of the vacuum chamber and mounted on a conflat flange with Viton O-rings. The FT-MS uses an electromagnet capable of 1.4 T, but these experiments were done at 0.8–1.0 T to enable detection of low-mass ions.

The cell configuration is roughly a 1-in. cubic cell except that the front and rear plates (transmitter plates) are separated by 1 1/2 in. The cell plates are made from polished oxygen-free copper (OFHC). For some of these experiments we also used molybdenum cell plates. The rear cell plate is a commercial copper mirror from SPAWR Optical Research with a stated reflectivity of 99% at 10.6 μm. The front cell plate contains a 15/16-in. hole covered by a 95% transmitting copper mesh with 29 lines/

in. These alterations allow laser light to pass into the cell and then be reflected collinearly back through the cell.

Pulsed laser photolysis was accomplished using the multimode output of a Lumonics TEA 103-2 CO<sub>2</sub> laser. The laser is line tunable using a grating element. We used a laser mixture containing nitrogen to achieve higher pulse energies. The temporal profile of the laser pulse (with nitrogen) consists of an initial high-intensity spike (about 80-ns fwhm) followed by a low-intensity tail extending for several microseconds (roughly 2-μs fwhm). The total energy is partitioned approximately equally between the spike and the tail. A Rofin 7400 photon drag detector and an Eltec 420-2 pyroelectric detector were used for the temporal profile measurements. A desired pulse energy is obtained by attenuating the laser beam with CaF<sub>2</sub> flats of varying thickness. The laser beam is weakly focused using a 10 m radius of curvature mirror located about 2.3 m from the FT-MS cell. An iris, located about 45 cm in front of the cell, provides the desired spot size. Intensity profile measurements with a pyroelectric detector indicate that this configuration gives a reasonable "top hat" profile at the location of the cell. The profile contains intensity variations because the laser is operated multimode to achieve higher pulse energies.

Pulse energies were measured using a Scientech 365 power and energy meter with a Scientech 38-0102 volume absorbing disk calorimeter. The laser beam spot size was measured just in front of the KCl window to the vacuum chamber by burn spots on thermal paper. Reported fluences were calculated by taking the pulse energy divided by the spot size and then multiplying by 2. We multiply by 2 because the laser beam is reflected back on itself so it passes through the cell twice and effectively doubles the number of photons compared to a single pass.

The pulsed laser misfires up to 5% of the time. The percentage of misfires is fairly reproducible on any given day. For this reason, we averaged at least 100 transients for any measurement so that the number of misfires would be reasonably constant between measurements.

Ions were also photolyzed using a home-built, grating-tuned, CW CO<sub>2</sub> laser. This laser provided about 12 W on the P(16) line of the 9.6-μm transition. Fluence can be controlled by changing the irradiation time with a Uniblitz shutter. Laser power was measured using an Optical Engineering 25-B power meter.

For both lasers, the laser wavelength was measured with an Optical Engineering 16-A CO<sub>2</sub> spectrum analyzer. IRMP dissociation was effected using the P(16) line of the 9.6-μm transition.

These experiments involved measuring branching ratios of ions with *m/z* 44 and 43. Under conditions similar to those of these experiments, we measured the isotope ratios for the CH<sub>2</sub>Cl<sup>+</sup> (*m/z* 49 and 51) fragment from methylene chloride to ensure quantitative accuracy. We consistently obtained a value of 3.1 ± 0.1, which agrees with natural isotopic abundances.<sup>37</sup>

**Calculations.** *Ab initio* molecular orbital calculations were performed using GAUSSIAN 90.<sup>38</sup> We started with the structures from the literature<sup>12</sup> and optimized with a 6-31G basis set to obtain harmonic vibrational frequencies for 1 and unlabeled 2. Structure 1 had only one negative frequency corresponding to the hydrogen atom transfer. We have used only these frequencies in our analysis and not the *ab initio* energetics. Optimizing with a different basis set had little effect, so that the previous *ab initio* study<sup>12</sup> can be consulted for structures. The frequencies were scaled by a factor<sup>39</sup> of 0.9.

RRKM calculations<sup>40–42</sup> (Appendix A) were performed using a program written in this laboratory.<sup>43</sup> Moments of inertia and rotational constants for the internal rotors were obtained from Gilbert's GEOM program.<sup>40</sup> Additional details concerning the RRKM program are provided elsewhere.<sup>44</sup>

(37) McLafferty, F. W. *Interpretation of Mass Spectra*, 3rd ed.; University Science Books: Mill Valley, CA, 1980.

(38) Frisch, M. J.; Head-Gordon, M.; Trucks, G. W.; Foresman, J. B.; Schlegel, H. B.; Raghavachari, K.; Robb, M. A.; Binkley, J. S.; Gonzalez, C.; Defrees, D. J.; Fox, D. J.; Whiteside, R. A.; Seeger, R.; Melius, C. F.; Baker, J.; Martin, R. L.; Kahn, L. R.; Stewart, J. J. P.; Topiol, S.; Pople, J. A. *GAUSSIAN 90*; Gaussian, Inc.: Pittsburgh, PA, 1990.

(39) Hehre, W. J.; Radom, L.; Schleyer, P. v. R.; Pople, J. A. *Ab Initio Molecular Orbital Theory*; Wiley: New York, 1986.

(40) Gilbert, R. G.; Smith, S. C. *Theory of Unimolecular and Recombination Reactions*; Blackwell Scientific Publications: Osney Mead, Oxford, U.K., 1990.

(41) Forst, W. *Theory of Unimolecular Reactions*; Academic Press: New York, 1973.

(42) Robinson, P. J.; Holbrook, K. A. *Unimolecular Reactions*; John Wiley and Sons Ltd.: New York, 1972.

(43) Wladkowski, B. W.; Lim, K. F.; Brauman, J. I. HYDRA. Department of Chemistry, Stanford University, 1991.

(29) Jasinski, J. M.; Rosenfeld, R. N.; Meyer, F. K.; Brauman, J. I. *J. Am. Chem. Soc.* **1982**, *104*, 652.

(30) Dunbar, R. C. *J. Chem. Phys.* **1991**, *95*, 2537.

(31) Marshall, A. G.; Verdun, F. R. *Fourier Transforms in NMR, Optical, and Mass Spectrometry: A User's Handbook*; Elsevier: New York, 1990.

(32) Marshall, A. G.; Grosshans, P. B. *Anal. Chem.* **1991**, *63*, 215.

(33) Grosshans, P. B.; Shields, P. J.; Marshall, A. G. *J. Chem. Phys.* **1991**, *94*, 5341.

(34) McIver, R. T. J.; Baykut, G.; Hunter, R. L. *Int. J. Mass. Spectrom. Ion Phys.* **1989**, *89*, 343.

(35) McIver, R. T. J.; Hunter, R. L.; Baykut, G. *Anal. Chem.* **1989**, *61*, 489.

(36) McIver, R. T. J.; Hunter, R. L.; Baykut, G. *Rev. Sci. Instrum.* **1989**, *60*, 400.

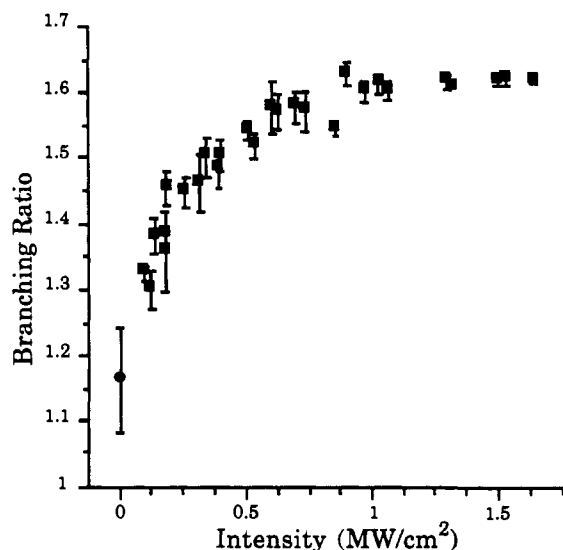


Figure 2. Branching ratio ( $^{13}\text{CH}_3\text{CO}^+/\text{CH}_3\text{CO}^+$ ) for pulsed (■) and CW (●) laser photolysis of **2**.

## Results

**CW Laser Photolysis.** The branching ratio for the CW laser photolysis of **2** =  $^{13}\text{CH}_3\text{CO}^+/\text{CH}_3\text{CO}^+$  =  $1.165 \pm 0.08$ . The intensity of the laser light was about  $40 \text{ W/cm}^2$ . The reported error is the standard deviation of five measurements, and each measurement involves averaging 1000 transients. The ions were irradiated for 400 ms. The total abundance of ions was the same in the "light on" and "light off" experiments. In other words, the sum of the product ion abundances and the unreacted parent ion abundance measured in the photolysis experiments was the same as the unreacted parent ion abundance when the laser was blocked. We refer to this as having mass balance.

**Pulsed Laser Photolysis.** Figure 2 gives branching ratios for the pulsed laser photolysis of **2**. The branching ratios range from 1.3 to 1.6. The intensity in Figure 2 is the intensity encountered in the tail of the laser pulse (see Appendix B). We have plotted the branching ratios versus intensity instead of fluence so we can also plot the CW laser branching ratio (the lowest intensity measurement). Fluences (in  $\text{J/cm}^2$ ) can be obtained by multiplying an intensity by  $4 \times 10^{-6} \text{ s}$ .<sup>45</sup> The reported errors are standard deviations of three to six measurements, and each measurement involves averaging 100–1200 transients. More transients are averaged for the lower intensity measurements. The branching ratios do not depend on the number of transients averaged. The points in Figure 2 came from data sets measured on 3 different days separated by up to 9 months. The mass balance is correct for intensities below about  $1.25 \text{ MW/cm}^2$ . The higher intensity measurements, however, have up to 15% ion loss.

**Background Reactivity.** We want to measure the amount of  $\text{CH}_3\text{CO}^+$  and  $^{13}\text{CH}_3\text{CO}^+$  produced by IRMP dissociation of **2**. This system contains background reactions which must be controlled to ensure accurate branching ratio measurements.

IRMP experiments at higher fluences and on  $\text{CH}_3\text{CO}^+$  formed directly by electron impact indicate that none of the primary IRMP products undergo secondary photochemistry.

The acetone enol cation reacts<sup>22</sup> with neutral 1-methylcyclobutanol to give  $\text{C}_5\text{H}_9^+$ , an ion with the molecular formula  $\text{M}+\text{C}_3\text{H}_5$ , and an ion with the molecular formula  $\text{M}+\text{C}_3\text{H}_4$  (where M is  $\text{C}_3\text{H}_6\text{O}$ ). These species can also undergo IRMP dissociation. The acetone enol cation can also react to form an ion with sufficient energy to fragment. That is, the acetone enol cation reacts with

neutral 1-([ $^{13}\text{C}$ ]methyl)cyclobutanol to form  $\text{CH}_3\text{CO}^+$  and  $^{13}\text{CH}_3\text{CO}^+$ . Control of these issues is discussed in two separate sections, one for the pulsed laser and one for the CW laser.

**Pulsed Laser.** Experiments were done at pressures ranging from  $2 \times 10^{-8}$  to  $4 \times 10^{-7}$  Torr. The acetone enol cation was isolated by standard notched ejection techniques. Fragments, which may have formed by background reactions, were ejected immediately (about 5 ms) before the laser pulse. The products were detected within 5–10 ms after the laser pulse. From the last ejection to the time of detection (about 15 ms in this case), a small amount of  $\text{CH}_3\text{CO}^+$  and  $^{13}\text{CH}_3\text{CO}^+$  will have formed by background reactions. To measure this, we took scans with the laser blocked and observed the amount of  $\text{CH}_3\text{CO}^+$  and  $^{13}\text{CH}_3\text{CO}^+$  formed. The amount was converted to a fraction of total ions and then used to correct the abundances of  $\text{CH}_3\text{CO}^+$  and  $^{13}\text{CH}_3\text{CO}^+$  for experiments with the laser light entering the cell. This correction must be made because the ions from background reactions have a different energy content and give different branching ratios. Very few  $\text{C}_5\text{H}_9^+$ ,  $\text{M}+\text{C}_3\text{H}_5$ , or  $\text{M}+\text{C}_3\text{H}_4$  ions form during the short time between their ejection and the detection of products, so we do not need to consider the photochemistry of these species with the pulsed laser experiments.

**CW Laser.** To minimize background reactions, experiments were done at pressures less than  $2 \times 10^{-8}$  Torr. Fragments were ejected immediately before laser irradiation and were detected as soon as possible after laser irradiation.  $\text{CH}_3\text{CO}^+$  and  $^{13}\text{CH}_3\text{CO}^+$  abundances were corrected with the same method used in the pulsed laser experiments. The acetone enol cation was irradiated for 400 ms. In that time, significant amounts of the  $\text{C}_5\text{H}_9^+$  ion and the  $\text{M}+\text{C}_3\text{H}_5$  ion can form (a very small amount of the  $\text{M}+\text{C}_3\text{H}_4$  ion also forms). These ions were continuously ejected during the laser pulse, so that they cannot also undergo IRMP dissociation. We use external circuitry to mix the frequency provided by the IonSpec data system with frequencies provided by function generators to permit more than one continuous ejection at the same time.

With the CW laser experiment we also must consider the possibility that the photoproducts may undergo reaction before detection. In this case we must assume that the products react with neutrals at the same rate, so that branching ratios will not be affected. This would be expected because the product ions only differ by a  $^{13}\text{C}$  label.

## Experimental Considerations

IRMP dissociation involves ions that dissociate after sequentially absorbing infrared photons. We use a  $\text{CO}_2$  laser, so the energy increment (energy of 1 photon) is about 3 kcal/mol, and therefore the ions dissociate over an energy range of at least 3 kcal/mol.<sup>46</sup> The activation process involves energy pumping, which in most cases occurs at a steady-state rate dependent on the intensity. Reaction starts to occur at the energy where the reaction rate competes with the pumping rate. Photolysis with a CW laser involves a pumping rate<sup>47</sup> of about  $10 \text{ s}^{-1}$ , so that the energy range for dissociation starts at the point where the lowest energy reaction has achieved a rate of  $10 \text{ s}^{-1}$ . This should occur essentially at the reaction threshold. Photolysis with the pulsed laser involves pumping rates of  $\sim 10^4\text{--}10^7 \text{ s}^{-1}$ , and some reactions may not achieve this rate except at energies significantly above their thresholds. Pulsed laser photolysis, therefore, can shift the energy range of dissociation to higher energies because an ion energized above the reaction threshold will absorb another photon if its reaction rate does not compete with the pumping rate. This process may also be limited by the length of the laser pulse. By measuring log reactant fluence (LRF) plots using Quack's

(44) Wladkowski, B. W.; Lim, K. F.; Allen, W. D.; Brauman, J. I. *J. Am. Chem. Soc.* **1992**, *114*, 9136.

(45) The tail of a laser pulse is approximately  $2 \mu\text{s}$  in length and contains approximately half of the photons of the entire laser pulse.

(46) Osterheld, T. H.; Brauman, J. I. *J. Am. Chem. Soc.* **1992**, *114*, 7158.

(47) This value comes from a fluence dependence study of acetone enol cation photolysis.

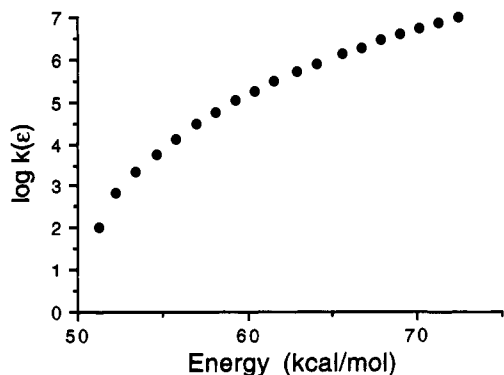


**Figure 3.** Dependence of the rate constant on energy for acetone enol cation isomerization as determined by RRKM calculations (Appendix A).

formalism, we can obtain estimates of pumping rates in the high-intensity spike of the laser pulse as well as the low-intensity tail.<sup>26-29</sup>

### Discussion

It has been shown convincingly that eq 1 is the reaction mechanism for methyl loss from the acetone enol cation.<sup>3,4,8-19</sup> Even though a "symmetrical" intermediate is formed the two methyl groups are lost at unequal rates. A previous metastable-ion measurement<sup>15</sup> of reaction 2 gives a branching ratio =  $^{13}\text{CH}_3\text{CO}^+/\text{CH}_3\text{CO}^+ = 1.36 \pm 0.15$ , demonstrating a preference for loss of the newly formed methyl group. This value has been independently confirmed<sup>5</sup> with a measured branching ratio of 1.4. A metastable-ion measurement<sup>15</sup> of the ion with the  $^{13}\text{C}$  label on the methylene carbon also gives a preference for loss of the newly formed methyl group. Measurements using deuterium labels give a branching ratio of 1.4 after correction for isotope effects.<sup>3,8</sup>

Typically, nonstatistical behavior has been demonstrated by converting an unsymmetrical reactant into a symmetric intermediate and observing that the "symmetric" intermediate decomposes unsymmetrically.<sup>1,2,48</sup> In the case of the acetone enol cation, it has been proposed that the acetone cation, formed with considerable energy by the isomerization (1), branches between losing the "hot" methyl group and undergoing ivr.<sup>3,19</sup> After ivr, the acetone cation loses both of the methyl groups statistically. The simplest picture, and the one posed previously,<sup>19</sup> is that a significant amount of the energy in the reaction coordinate is deposited by the transferring hydrogen into the antisymmetric stretch involving the newly formed methyl group. The large amount of energy in this mode can cause the bond to break before the energy can be randomized. Our results require this minimal description to be further elaborated, because it is not consistent with the strong (at least at energies near the reaction threshold) energy dependence of the nonstatistical reaction (vide infra). It appears that another mode of 1 influences the amount of nonstatistical dissociation.

Our IRMP dissociation experiments 2 also show selectivity (Figure 2), confirming the nonstatistical dissociation behavior. Because IRMP activation involves pumping energy into the ion in competition with other processes, we can activate to a relatively narrow energy range. By changing laser intensity, we can roughly control the energy at which ions dissociate. Using the CW laser allows us to study reactions occurring at much slower rates and at lower energies than those studied with other techniques.

To better quantify the reaction behavior, we have used RRKM theory to calculate rates for the first step of reaction 1 (Appendix A). The rate constants as a function of energy are plotted in Figure 3. We calculated rate constants using different barrier heights to determine a critical energy. Using a critical energy of 51.0 kcal/mol, we obtained a rate<sup>49,50</sup> of  $10^4 \text{ s}^{-1}$  for the minimum

**Table I.** Dependence of Branching Ratios (Nonstatistical Dissociation) on Energy<sup>a</sup>

measurement	energy above barrier <sup>b</sup>	energy content of 3 <sup>b</sup>	branching ratio	fraction nonstatistical <sup>c</sup>
CW laser	0-3	37-40	1.165	0.076
metastable ion <sup>d</sup>	4-14 (~8) <sup>e</sup>	41-51 (~45) <sup>e</sup>	1.36	0.15
pulsed laser <sup>f</sup>	~8-12	45-49	1.55	0.22

<sup>a</sup> Isomerization barrier of 51.0 kcal/mol. <sup>b</sup> In kcal/mol. <sup>c</sup> Assumes that loss of original methyl is completely statistical. <sup>d</sup> Reference 15. <sup>e</sup> For reaction rate of  $1 \times 10^5 \text{ s}^{-1}$ . <sup>f</sup> Fluence of  $2.5 \text{ J/cm}^2$ .

energy at which the reaction is experimentally observed, thus correcting for the kinetic shift.<sup>51,52</sup> In other words, the experimental determination should be larger than the actual critical energy because only reactions occurring faster than  $10^4 \text{ s}^{-1}$  can be observed in the metastable ion.

Table I gives the nonstatistical reaction behavior as a function of energy. For the CW laser, we assume that the reaction energy range starts at the threshold and spans the energy of one photon (3 kcal/mol). For the metastable ion, we give the energy range for reaction rate constants<sup>49,50</sup> of  $10^4$ - $10^6 \text{ s}^{-1}$  as well as the energy for a reaction rate constant of  $10^5 \text{ s}^{-1}$  (which we assume corresponds to the most probable reaction rate constant). For the pulsed laser, we used the analysis in Appendix B to determine pumping rates and energies for dissociation from a  $2.5 \text{ J/cm}^2$  laser pulse (this corresponds to an intensity of  $0.625 \text{ MW/cm}^2$  in Figure 2). The fraction of nonstatistical dissociation comes from assuming that all reactions giving loss of the *original* (spectator) methyl group in 2 occur statistically and that the two methyl groups are lost at equal rates for the statistical reaction. This assumption is probably not completely correct.<sup>13,19</sup>

It is clear that increasing the energy at which the isomerization occurs results in significantly more nonstatistical dissociation.<sup>53</sup> The magnitude of the dependence is quite surprising for several reasons. (1) Activation near the threshold (CW laser) only gives a small amount of nonstatistical dissociation (branching ratio = 1.17) even though the reaction coordinate still provides energy in considerable excess of that required to subsequently break the carbon-carbon bond. (2) Because the energy in excess of the isomerization barrier should be statistically distributed among all of the modes, activation with the pulsed laser<sup>54</sup> compared to the CW laser should not involve that much more energy *in the reaction coordinate*. (3) The higher energy reaction from the pulsed laser only provides an incremental increase of an already large value (i.e., even with the CW laser, at least 37 kcal/mol of energy is deposited from the reaction coordinate into 3). Yet activation with the pulsed laser gives significantly more nonstatistical dissociation than activation with the CW laser. These observations indicate that excitation of another mode in 1 (the transition state) influences the amount of nonstatistical decomposition. For example, consider an ion reacting with 51.5 kcal/mol of energy (the CW laser gives ions with 51.0-54.0 kcal/mol). An energy of 51.0 kcal/mol is required in the reaction coordinate for isomerization, and 0.5 kcal/mol is available for other modes. Only the torsion of the spectator methyl group has a frequency sufficiently low to take up any excess energy; the other modes cannot be excited. In this situation, little nonstatistical dissociation appears to occur even though the system has

(49) Burgers, P. C.; Holmes, J. L. *Org. Mass. Spectrom.* **1982**, *17*, 123.

(50) Williams, D. H. *Acc. Chem. Res.* **1977**, *10*, 280.

(51) Chupka, W. A. *J. Chem. Phys.* **1959**, *30*, 191.

(52) Lifshitz, C. *Mass Spectrom. Rev.* **1982**, *1*, 309.

(53) This agrees with a previous study (see ref 8). The previous study, however, involved average energies that were significantly higher than the energies in our work as well as energies that were not easily characterized. The previous study also involved some ions with sufficient energy to cleave the bond to the spectator methyl group of the acetone enol cation.

(54) We could also make comparisons between the CW laser photolysis and the metastable-ion results.

(48) Rynbrandt, J. D.; Rabinovitch, B. S. *J. Phys. Chem.* **1970**, *74*, 4175.

considerable energy in the reaction coordinate. Now consider reactions occurring around 54.0 kcal/mol or higher (at the upper end of CW laser activation). In this case, other modes of **1** can be excited. It is at this point that the amount of nonstatistical dissociation appears to increase.

It is not unreasonable that another mode might influence the amount of nonstatistical dissociation. Excitation of a C–C–O bend in **1** (involving the *spectator* methyl moiety) may facilitate the nonstatistical reaction leading to the observed behavior. In the loss of the methyl radical from the acetone cation, the reaction involves converting the bent C–C–O bond angle into a linear bond angle because the heavy-atom framework of the acetyl cation is linear.<sup>12,24</sup> We would therefore expect that the reaction coordinate would involve some excitation of this C–C–O bend in addition to the antisymmetric motion of the carbons. While the isomerization of the acetone enol cation to the acetone cation would deposit significant energy into the antisymmetric stretch of the carbons, it might not initially deposit energy into the C–C–O bend. The strong energy dependence of the nonstatistical dissociation may therefore arise because, at higher energies, more ions pass through the isomerization transition state with the C–C–O bend of **1** excited. This leads to an acetone cation completely prepared to dissociate by having energy in the antisymmetric stretch to expel the newly formed methyl group and energy in the C–C–O bend involving the spectator methyl carbon.<sup>55</sup> The properly prepared acetone cation may dissociate prior to ivr whereas the ion formed without the C–C–O bend already excited must undergo ivr in order to deposit energy into the C–C–O bend.

The acetone cation has an electronically excited state that lies about 51 kcal/mol above its ground electronic state (at an energy of 65 kcal/mol in Figure 1).<sup>56</sup> It has been suggested that the acetone enol cation can isomerize to form the acetone cation in this excited state and that the excited state is involved in the nonstatistical dissociation.<sup>19</sup> Some dissociations occurring in the metastable-ion time frame might have sufficient energy to involve the excited state. Our IRMP dissociation experiments with the CW laser appear to rule out this possibility. Our experiments involve reactions occurring at energies just above the isomerization barrier but well below the threshold for formation of the excited state. We still observe a nonstatistical branching ratio in our CW laser experiments.

**Conclusion.** The energy dependence of the nonstatistical dissociation of the acetone enol cation has been studied using IRMP dissociation techniques in an FT-MS. These experiments reveal a surprisingly strong energy dependence for the amount of nonstatistical reaction. The implication is that another mode in the transition state for isomerization of the acetone enol cation to the acetone cation affects the amount of nonstatistical reaction. A mode involving a C–C–O bend of the spectator methyl group carbon has been suggested as a candidate.

**Acknowledgment.** We are grateful to the National Science Foundation for support of this work. We thank Professor Richard N. Zare for insights and helpful discussions, and we are grateful to Professor Robert McIver and Dr. Richard Hunter of IonSpec for considerable technical help. T.H.O. gratefully acknowledges graduate fellowship support from the W. R. Grace Foundation.

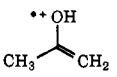
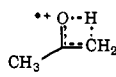
#### Appendix A. RRKM Calculations

The parameters for reaction 1 are given in Table II. The frequencies were obtained from *ab initio* calculations with a 6-31G basis set and are for the ion that does not have a <sup>13</sup>C label. The frequencies were scaled

(55) This mechanism for the nonstatistical dissociation is consistent with the observation of Lifshitz and co-workers that metastable loss of the original methyl group is also bimodal (see refs 13 and 19). Recoil of the antisymmetric stretch would result in the correct arrangement to expel the original methyl group, and presumably, the C–C–O bend involving the newly formed methyl group would already be excited.

(56) Qian, K.; Shukla, A.; Futrell, J. J. *Chem. Phys.* **1990**, *92*, 5988.

Table II. RRKM Parameters for Reaction 1<sup>a</sup>

					
3515	1452	871	3069	1419	912
3138	1444	809	3001	1379	834
3019	1408	676	2958	1326	591
3009	1387	521	2926	1285	441
2931	1087	470	2864	1124	351
2868	1060	393	1684	1037	350
1521	1047	353	1463	1017	
1463	1005		1428	957	
$B_{\text{ext}}(\text{inact}), \sigma_1 0.3205, 1 (1)^b$			$B_{\text{ext}}(\text{inact}), \sigma_1 0.3291, 1 (1)$		
$B_{\text{ext}}(\text{act}), \sigma_1 0.16445, 1 (1)$			$B_{\text{ext}}(\text{act}), \sigma_1 0.1684, 1 (1)$		
$B_{\text{int}}, \sigma_1 8.163, 3 (1)$			$B_{\text{int}}, \sigma_1 7.085, 3 (1)$		

<sup>a</sup> Frequencies and rotational constants are in units of cm<sup>-1</sup>. <sup>b</sup> Dimension of rotor.

by a factor<sup>39</sup> of 0.9. We obtained the rotational constants for the torsions from Gilbert's GEOM program.<sup>40</sup>

We used a critical energy for reaction 2 of 51.0 kcal/mol. This gives a reaction rate of  $9 \times 10^3 \text{ s}^{-1}$  at 55.0 kcal/mol, which is the minimum energy at which methyl loss can be observed in a metastable-ion measurement.<sup>18</sup> Metastable ions require a minimum rate<sup>49,50</sup> of about  $10^4 \text{ s}^{-1}$ , so we have simply corrected for the kinetic shift.<sup>51,52</sup>

For the calculations reported in this paper, we did not explicitly consider conservation of orbital angular momentum. Conserving orbital angular momentum should only have a relatively small effect because the external moments do not change greatly in an isomerization (compared to a dissociation).

#### Appendix B. Determination of the Dissociation Energy Range from Pulsed Laser Photolysis

The IRMP activation process involves a competition between the rate for photon absorption and the rate for reaction. When a reaction rate exceeds the pumping rate, dissociation will start to occur. Because the critical energy is so high and the reaction involves a tight transition state, an ion must absorb several photons above threshold to reach energies where the dissociation rates (Figure 3) approach the pumping rates. In this case, the length of the laser pulse can also limit how many photons are absorbed.<sup>57</sup> It appears that the number of photons in the initial high-intensity spike is too small for a significant number of ions to absorb sufficient photons to reach a competitive reaction rate. Thus, a competitive reaction rate is only reached toward the end of the entire laser pulse.<sup>57</sup> We have modeled the photolysis by assuming that the energy at which most ions dissociate is determined by the pumping rate in the low-intensity tail, which is the latter part of the laser pulse. This model appears to work well for comparisons to metastable ions (vide infra).

Our IRMP dissociation experiments give a branching ratio of 1.4 at an intensity of 0.25 MW/cm<sup>2</sup> (fluence of 1.0 J/cm<sup>2</sup>). We can estimate the pumping rate for this intensity by using Quack's formalism.<sup>26-29</sup> The rate coefficient<sup>26-29</sup> from an LRF plot is 0.124 cm<sup>2</sup>/J. For the 2- $\mu\text{s}$  tail, the pumping rate is  $0.25 \times 10^6 \text{ W/cm}^2 \times 0.124 \text{ cm}^2/\text{J} = 3.1 \times 10^4 \text{ s}^{-1}$ . This corresponds to the rate for isomerization at an energy of 6 kcal/mol above the barrier. The energy range for dissociation, therefore, is 6–9 kcal/mol above the barrier (one photon is the energy equivalent of 3 kcal/mol). This comes from the approximation that ions below 6 kcal/mol absorb another photon and ions above do not.

Fortunately, we can make comparisons to metastable-ion results to calibrate our analysis. Metastable-ion experiments in **2** also give a branching ratio of 1.4. We assume that the most probable rate in metastable ions<sup>52</sup> is  $1 \times 10^5 \text{ s}^{-1}$ . From our RRKM calculation, the energy at which the isomerization has a rate of  $1 \times 10^5 \text{ s}^{-1}$  is 8.2 kcal/mol above the threshold. This is in reasonable agreement with our determination from the IRMP dissociation experiment but is slightly higher than the average energy of the IRMP dissociation range. We would not be surprised if our estimate of the IRMP pumping rate was slightly low. The amount of overall dissociation for a constant fluence appeared to have some dependence on the delay after ion formation consistent with a minor pumping bottleneck. We can adjust our coefficient to account for the difference by assuming that a 0.25 MW/cm<sup>2</sup> laser pulse should give an

(57) Han, C.-C.; Brauman, J. I. *J. Phys. Chem.* **1990**, *94*, 3403.

average energy of 8.2 kcal/mol (energy range of 6.7–9.7 kcal/mol). The RRKM rate at 6.7 kcal/mol is  $4.8 \times 10^4 \text{ s}^{-1}$ , which yields a corrected coefficient of 0.192 cm<sup>2</sup>/J. We will compare the results using this coefficient with results using the coefficient from the LRF plot.

We want to obtain the energy range of reaction for a 0.625 MW/cm<sup>2</sup> laser pulse (fluence of 2.5 J/cm<sup>2</sup> in Table I). For the 2- $\mu$ s tail, the pumping rate is  $0.625 \times 10^6 \text{ W/cm}^2 \times 0.124 \text{ cm}^2/\text{J} = 7.75 \times 10^4 \text{ s}^{-1}$ . This corresponds to the rate for isomerization at an energy of 7.6 kcal/mol above the barrier. Therefore, the energy range for dissociation of 7.6–10.6 kcal/mol. We can also use the bimolecular rate coefficient calibrated with the metastable ion experiments. For the 2- $\mu$ s tail, the pumping rate is  $0.625 \times 10^6 \text{ W/cm}^2 \times 0.192 \text{ cm}^2/\text{J} = 1.2 \times 10^5 \text{ s}^{-1}$ . This corresponds to the rate for isomerization at an energy of 8.5 kcal/mol above the

barrier. In this analysis, the energy range for dissociation is 8.5–11.5 kcal/mol. We therefore estimate that the energy range for dissociation from a 2.5 J/cm<sup>2</sup> laser pulse is about 8–12 kcal/mol and realize that this result is a rough approximation.

The conclusions in our study are drawn from the observation that the branching ratios increase significantly with energy. Our analysis of reaction energies must be reasonably accurate on the basis of the comparison to experiments with metastable ions. Even if the pulsed laser photolysis at 2.5 J/cm<sup>2</sup> involved the absorption of more photons than we have calculated, our conclusions would not change. For example, absorbing two more photons would put the energy range at only 14–18 kcal/mol, which is still a small amount of energy relative to the total exothermicity.